

Quantum charge pumping through a superconducting double barrier structure in graphene

Arijit Kundu¹, Sumathi Rao² and Arijit Saha³

¹ *Institut für Theoretische Physik, Heinrich-Heine-Universität, D-40225 Düsseldorf, Germany*

² *Harish-Chandra Research Institute, Chhatnag Road, Jhusi, Allahabad 211019, India*

³ *Department of Condensed Matter Physics, Weizmann Institute of Science, Rehovot 76100, Israel*

(Dated: May 30, 2022)

We consider the phenomenon of quantum charge pumping of electrons across a superconducting double barrier structure in graphene in the adiabatic limit. In this geometry, quantum charge pumping can be achieved by modulating the amplitudes (Δ_1 and Δ_2) of the gaps associated with the two superconducting strips. We show that the superconducting gaps give rise to a transmission resonance in the Δ_1 - Δ_2 plane, resulting in a large value of pumped charge, when the pumping contour encloses the resonance. This is in sharp contrast to the case of charge pumping in a normal double barrier structure in graphene, where the pumped charge is very small, due to the phenomenon of Klein tunneling. We analyse the behaviour of the pumped charge through the superconducting double barrier geometry as a function of the pumping strength and the phase difference between the two pumping parameters, for various angles of the incident electron.

PACS numbers: 73.23.-b, 72.80.Vp, 74.45.+c

I. INTRODUCTION

The phenomenon of quantum charge pumping corresponds to a net flow of DC current between different electron reservoirs (at zero bias) connected via a quantum system whose parameters are periodically modulated in time¹⁻³. The zero-bias current is obtained in response to the time variation of the parameters of the quantum system, which explicitly break time-reversal symmetry. It is necessary to break time-reversal symmetry in order to get net pumped charge, but it is not a sufficient condition. For obtaining a net pumped charge, parity or spatial symmetry must also be broken. Within a scattering approach, if the time period of modulation of the scattering system parameters is much larger than the time the particle spends inside the scattering region (dwell time), the adiabatic limit is reached. In this limit, the pumped charge in a unit cycle becomes independent of the pumping frequency. This is referred to as “adiabatic charge pumping”³. In recent years, quantum charge and spin pumping through various mesoscopic samples, involving quantum dots and quantum wires, have attracted increasing interest both theoretically⁴⁻¹⁶ and experimentally¹⁷⁻²¹, both in the adiabatic regime and otherwise.

The discovery of graphene, a two dimensional single layer of graphite, by K. S. Novoselov *et al.*²² a few years ago, has led to an upsurge in the study of its transport properties, both theoretically and experimentally²³⁻²⁵. The low energy quasiparticle excitations in graphene behave like massless relativistic Dirac fermions. This provides us with an experimental test bed for observing many well-known phenomena in relativistic quantum mechanics, such as the Klein paradox²⁶ at low energies. In the recent past, a graphene-based quantum pump has been considered in literature²⁷⁻²⁹ where pumped charge is obtained in an adiabatic quantum pump device based

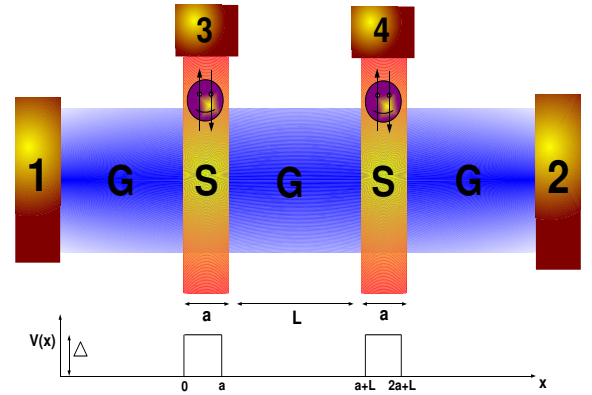


FIG. 1: (Color online) Cartoon of the SDB structure where a graphene sheet is connected to two reservoirs labeled 1 and 2. Superconducting material is deposited on top of the two patches labeled S and connected to contacts labeled 3 and 4. The schematic of the potential profile seen by an incident electron is shown below.

on a graphene monolayer modulated by two oscillating gate potentials. However, the pumped charge obtained in these kind of devices is quite small.

Quantum charge pumps, using a variety of setups involving superconductors, have also been of major interest in recent years³⁰⁻⁴⁰. Also, very recently, adiabatic charge pumping in graphene with superconductors has also been considered⁴¹. However an adiabatic quantum pump device based on superconducting double barrier (SDB) structures in graphene⁴² has not yet been considered in the literature. Motivated by this fact, in this article we consider quantum pumping of electrons (in the adiabatic limit) across an SDB structure in graphene, as

depicted in Fig. 1. Till date, no experiment has been carried out in the context of charge pumping with superconducting barriers. Experimentally it might be possible to design an SDB structure by depositing thin strips of superconducting material on top of a single ballistic 2D graphene sheet at two places. This can induce a finite superconducting gap in the barrier regions of the graphene sample due to the proximity of the superconducting strips. In principle, we can explore two scenarios to achieve significant amount of pumped charge – (a) by periodic modulation of amplitudes Δ_1 and Δ_2 of the gaps at the two superconducting barriers (SB) or alternatively, (b) by periodic modulation of the order parameter phases ϕ_1 and ϕ_2 associated with the two barriers. In this paper, we explore the first alternative, since it has been seen in earlier work⁴⁰ that the second alternative leads to less pumped charge. For free electrons in the graphene sheet, we show that in the $\Delta_1 - \Delta_2$ plane, there is a sharp resonance point in the transmission probability across the SDB structure. This is in sharp contrast to the case of charge pumping in a normal DB structure in graphene where the transmission probability across the DB structure does not have any resonance structure due to the phenomenon of Klein tunneling. In the SDB geometry, when we consider Δ_1 and Δ_2 as the pumping parameters, we can always choose a pumping contour which completely encloses the transmission resonance. Hence it is possible for the pumped charge to be large if the resonance is sharp enough.

This paper is organized as follows. In Sec. II, we discuss the theoretical modelling of the SDB structure in graphene and describe the resonance structure in the pumping parameter $\Delta_1 - \Delta_2$ plane. In Sec. III, we discuss the numerical results for the pumped charge as a function of the various parameters in the theory and also contrast it with that of normal DB geometry. Finally in Sec. IV, we present our summary and conclusions.

II. RESONANT TRANSMISSION IN GRAPHENE SDB STRUCTURE

Quantum transport in the SDB structure in graphene was considered recently in Ref. 42. Here we consider the same set-up, but instead of applying a bias across terminals 1 and 2, we shall use terminals 3 and 4 to change the amplitudes of the superconducting barriers in a time-dependent and out of phase fashion. The SDB structure is formed by depositing thin strips of superconducting material on top of the graphene sheet at two places. This induces a finite superconducting gap ($\Delta_i e^{i\phi_i}$) in the barrier regions as a result of the proximity effect. (i refers to the index of the strips). The geometry is shown in Fig. 1. The spatial dependence of the order parameter (which also acts as a scattering potential for the incident

electron) can be expressed as

$$V(x) = \Delta e^{i\phi} \Theta(x) \Theta(-x+a) + \Delta e^{i\phi} \Theta[x - (a+L)] \Theta[-x + (2a+L)] \quad (1)$$

where a is the width of the superconducting barrier and L is the distance between the two barriers. Here we assume that the spatial variation of the potential steps is slow on the scale of the lattice spacing so that inter-valley scattering is suppressed. Θ is the Heaviside Θ -function, and we have taken $\phi_1 = \phi_2 = \phi$, since we will not be looking at supercurrents (Josephson effect) in this work.

Following Ref. 42, we use a four dimensional version of the Dirac-Bogoliubov-de Gennes equation (DBDG)⁴³ for electrons and holes which is given by

$$\begin{pmatrix} \vec{k} \cdot \vec{\sigma} - U & \Delta \\ \Delta^* & -(\vec{k} \cdot \vec{\sigma} - U) \end{pmatrix} \begin{pmatrix} u \\ v \end{pmatrix} = \epsilon \begin{pmatrix} u \\ v \end{pmatrix} \quad (2)$$

where, $U = U(\mathbf{r}) + E_F$, and the energy ϵ is measured from the Fermi level of the superconductor. We assume that $U(\mathbf{r}) = 0$ in the normal graphene region and $U(\mathbf{r}) = U_0$, a constant, independent of \mathbf{r} in the proximity induced superconducting region. Note that we have defined dimensionless variables

$$\begin{aligned} x &\Rightarrow \frac{x E_F}{\hbar v_F}, & y &\Rightarrow \frac{y E_F}{\hbar v_F}, & k_y &\Rightarrow \frac{\hbar v_F k_y}{E_F}, \\ \Delta &\Rightarrow \frac{\Delta}{E_F}, & \epsilon &\Rightarrow \frac{\epsilon}{E_F} & \text{and } U &\Rightarrow \frac{U}{E_F} \end{aligned} \quad (3)$$

to replace the original ones.

The solution of the DBDG equations⁴³, describing electrons and holes with incident energy ϵ inside the normal graphene regions ($\Delta_{(i)} = 0$), can be written as

$$\Psi^{e\pm} = \frac{e^{ik_y y \pm ik_x x}}{\sqrt{\cos \alpha}} \begin{pmatrix} e^{\mp i\alpha/2} \\ \pm e^{\pm i\alpha/2} \\ 0 \\ 0 \end{pmatrix} \quad (4)$$

$$\Psi^{h\pm} = \frac{e^{ik_y y \pm ik'_x x}}{\sqrt{\cos \alpha'}} \begin{pmatrix} 0 \\ 0 \\ e^{\mp i\alpha'/2} \\ \mp e^{\pm i\alpha'/2} \end{pmatrix} \quad (5)$$

where $\alpha = \sin^{-1}[k_y/(\epsilon+1)]$, $\alpha' = \sin^{-1}[k_y/(\epsilon-1)]$, $k = \sqrt{\epsilon^2 - k_y^2}$ and $k' = \sqrt{\epsilon^2 - k_y^2}$. α is the angle of incidence of the incoming electron (with wave-vector (k, k_y)) and α' is the angle of reflection of the Andreev reflected hole (with wave-vector (k', k_y)). For retro Andreev reflection (AR), α', k' have opposite signs from α, k whereas for specular Andreev reflection (SAR), they have the same signs. The change from retro AR ($\epsilon < 1$) to SAR ($\epsilon > 1$) occurs at $\epsilon = 1$ (in our dimensionless units).

Similarly for the superconducting barrier regions, the four component spinor solutions (u, v) contain electron wave-functions u of one valley and hole wave-functions

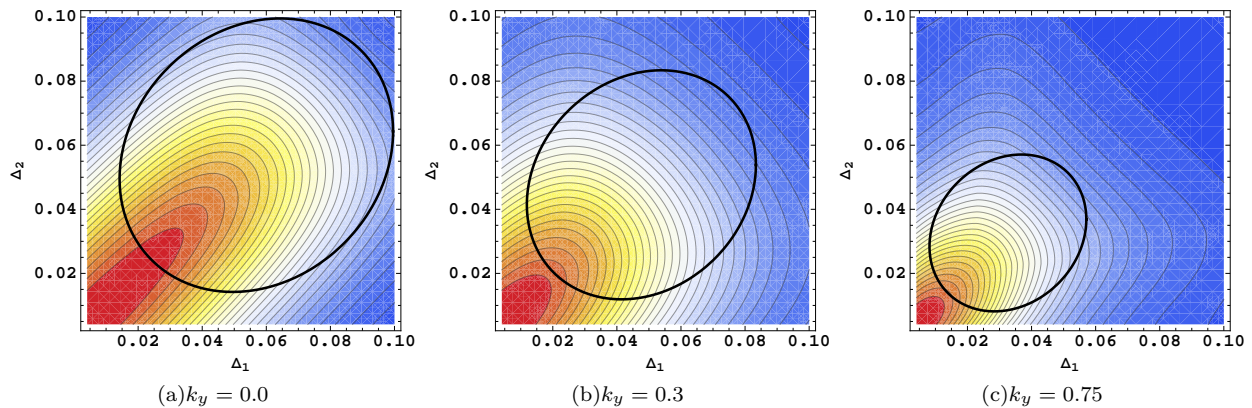


FIG. 2: (Color online) Contours of the transmission probability $|t_c|^2$ in the $\Delta_1 - \Delta_2$ plane for three different values of k_y . The steps between the maxima and minima of $|t_c|^2$ range approximately 1.0 to 0.1, 0.6 to 0.05 and 0.3 to 0.01 for the three cases $k_y = 0.0, 0.3$ and 0.75 respectively. In (a), (b) and (c) $a/L = 0.017, \Delta_0 = 40.0, U_0 = 10.0, \phi_1 = \phi_2 = 0.0$ and $\epsilon = 0.00142, 0.00121, 0.00082$ for the three contour plots respectively. The black circle represents the pumping contour for the parameter values $\omega = 1.0, P = 30.0$ and $\eta = 4\pi/9$.

v of the other valley. The DBDG equation can now be solved for any arbitrary energy ϵ and the four solutions inside the superconducting barriers are given in the preprint version of Ref. 43

$$\psi_{1/2} = e^{ik_y y \pm x \sqrt{k_y^2 - (U + \sqrt{(\epsilon^2 - \Delta^2)})^2}} \begin{pmatrix} e^{i\beta} \\ \pm e^{i\beta \pm i\gamma_1} \\ e^{-i\phi} \\ \pm e^{-i\phi \pm i\gamma_1} \end{pmatrix} \quad (6)$$

$$\psi_{3/4} = e^{ik_y y \pm x \sqrt{k_y^2 - (U - \sqrt{(\epsilon^2 - \Delta^2)})^2}} \begin{pmatrix} e^{-i\beta} \\ \pm e^{-i\beta \pm i\gamma_2} \\ e^{-i\phi} \\ \pm e^{-i\phi \pm i\gamma_2} \end{pmatrix} \quad (7)$$

where the subscripts 1/2 refers to the upper and lower signs on the RHS respectively, and similarly for 3/4 and

$$\begin{aligned} \gamma_1 &= \sin^{-1} \left(\frac{k_y}{U + \sqrt{(\epsilon^2 - \Delta^2)}} \right) \\ \gamma_2 &= \sin^{-1} \left(\frac{k_y}{U - \sqrt{(\epsilon^2 - \Delta^2)}} \right) \end{aligned} \quad (8)$$

and

$$\begin{aligned} \beta &= \cos^{-1} \frac{\epsilon}{\Delta} \quad \text{if } \epsilon < \Delta \\ &= -i \cosh^{-1} \frac{\epsilon}{\Delta} \quad \text{if } \epsilon > \Delta. \end{aligned} \quad (9)$$

Here, we have not taken the limit $U \gg \Delta, \epsilon$. We have also obtained the solution for both right-moving and left-moving electrons and holes.

Solving the BdG equation in the normal and superconducting regions, we obtain the net quantum mechanical amplitudes for reflection, transmission (co-tunneling (CT)), AR (and SAR) and crossed Andreev reflection

(CAR) (and specular crossed Andreev reflection (SCAR)) of an electron incident on the SDB structure, after it has traversed both the barriers.

In the non-relativistic case, a DB structure always lead to resonances and this affects the transmissions and the reflections through the system. For relativistic electrons, the standard paradigm is that one cannot obtain confined carrier states for normal incidence^{26,43} due to Klein tunneling. However, for relativistic electrons with superconducting barriers, even for normal incidence, discrete Andreev bound levels can clearly lead to resonant transmissions in a SDB structure in graphene⁴².

Here we use the standard wave-function matching technique to solve such scattering problems to obtain all the four quantum mechanical amplitudes across the SDB geometry in graphene. To the left of the SDB structure, with an incident electron from the left, the wave-function can be written as

$$\psi^{e+} + r_c \psi^{e-} + r_{Ac} \psi^{h-} \quad (10)$$

and to the right of the SDB structure, the wave-function can be written as

$$t_c \psi^{e+} + t_{Ac} \psi^{h+}. \quad (11)$$

Hence matching the wavefunctions in the normal and proximity induced superconducting regions (Eq.(4-7)) at the four normal-superconductor (NS) interfaces ($x = 0, a, a + L, 2a + L$) forming the SDB structure, we obtain sixteen linear equations. Numerically solving these sixteen equations, we obtain the four amplitudes r_c, r_{Ac}, t_c and t_{Ac} , for the SDB structure, for an incident electron with energy ϵ below the gap Δ ⁴². Here r_c is the reflection amplitude, r_{Ac} is the AR (and SAR) amplitude, t_c is the CT amplitude and t_{Ac} is the CAR (and SCAR) amplitude. Note that we distinguish between electron and hole parameters, and hence the four amplitudes will be different

for incident electrons and holes. Moreover, in our numerical analysis we do not distinguish between specular and retro Andreev reflections.

III. NUMERICAL RESULTS FOR THE PUMPED CHARGE

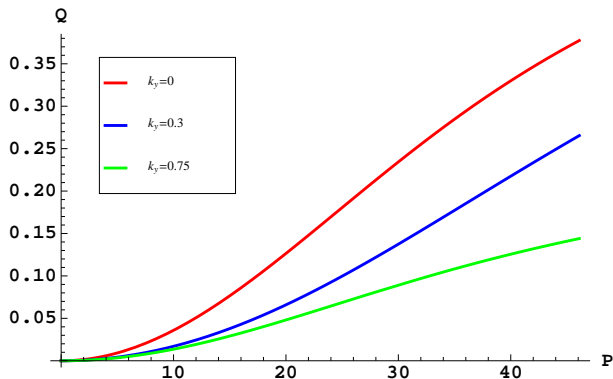


FIG. 3: (Color online) The value of the pumped charge Q in units of electron charge e , for pumping in $\Delta_1 - \Delta_2$ plane, is shown as a function of the pumping strength P for three different values of k_y . Here $a/L = 0.017, \omega = 1.0, \eta = 4\pi/9, \Delta_0 = 40.0, U_0 = 10.0, \phi_1 = \phi_2 = 0.0$ and $\epsilon = 0.00142, 0.00121, 0.00082$ for the three plots respectively.

In our numerical analysis for calculating the pumped charge through the SDB structure, we choose the amplitudes of the order parameters of the two superconducting strips (Δ_1 and Δ_2) as our pumping parameters. Here, Δ_1 and Δ_2 are taken to oscillate with the frequency ω , with a modulation parameter P , and a phase difference 2η between them, *i.e.*, we choose

$$\begin{aligned}\Delta_1 &= [\Delta_0 + P \cos(\omega t + \eta)]\epsilon \\ \Delta_2 &= [\Delta_0 + P \cos(\omega t - \eta)]\epsilon.\end{aligned}\quad (12)$$

$\Delta_0\epsilon$ is the mean value of the amplitude around which the two pumping parameters are modulated with time and P is called the pumping strength. Here ϵ is the energy of the incident electron. It is adjusted to be close to an Andreev bound level, so that the SDB is close to a resonance. Hence, effectively by varying P , for fixed ϵ we vary the ratio ϵ/Δ . By fixing ϵ to be close to the resonance, we maximise the pumped charge. The presence of two time-varying potentials with a phase difference between them explicitly violates parity, which is a necessary condition for obtaining pumped charge. The frequency of the potential modulation is kept small in comparison to the characteristic times for traversal and reflection, so that the pump is in the adiabatic limit.

In Fig. 2(a), we plot the transmission probability ($|t_c|^2$) in the $\Delta_1 - \Delta_2$ plane for various values of the transverse electron momentum k_y . Unlike the case of normal DB, where there is no resonance because of the phenomenon of Klein tunneling, for the SDB, $|t_c|^2 = 1$ resonance does

occur for normal incidence of electrons, *i.e.* $k_y = 0$. These bound states are produced due to the superposition of both electron and hole states and not just from any one of them. Hence these resonances are also different from the resonances that occur in normal double barriers in other materials. For nonzero values of k_y , $|t_c|^2 = 1$ gets damped as normal reflection and CAR (and SCAR) also take part in transport with nonzero values⁴² as shown in Figs. 2(b) and (c).

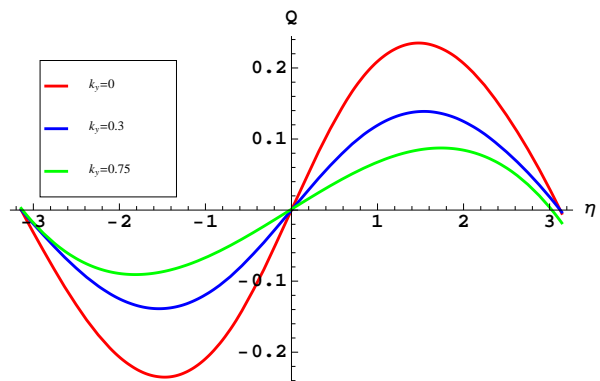


FIG. 4: (Color online) The value of the pumped charge Q in units of electron charge e , for pumping in $\Delta_1 - \Delta_2$ plane, is shown as a function of the phase difference between the two pumping parameters η for three different values of k_y . Here $a/L = 0.017, \omega = 1.0, P = 30.0, \Delta_0 = 40.0, U_0 = 10.0, \phi_1 = \phi_2 = 0.0$ and $\epsilon = 0.00142, 0.00121, 0.00082$ for the three plots respectively.

Using the modified version of the Brouwer's formula^{3,39,40}, the pumped charge through the graphene SDB structure can directly be obtained from the parametric derivatives of the \mathcal{S} -matrix elements. For a single channel \mathcal{S} -matrix, we have

$$Q = \frac{e}{2\pi} \int_0^\tau dt \left[\left(|r_c|^2 \dot{\theta} + |t_c|^2 \dot{\chi} \right) \cos \alpha - \left(|r_{Ac}|^2 \dot{\beta} + |t_{Ac}|^2 \dot{\gamma} \right) \cos \alpha' \right] \quad (13)$$

where θ , χ , β and γ correspond to the phases of the reflection, transmission, AR (and SAR) and CAR (and SCAR) amplitudes respectively. Note the negative sign in Eq.13, which results from the fact that r_{Ac} and t_{Ac} correspond to the conversion of an electron into a hole. Thus, the pumped charge through the SDB structure in graphene is directly related to the amplitudes and phases that appear in the \mathcal{S} -matrix. Inserting the unitarity relation $|r_c|^2 + |t_c|^2 + |r_{Ac}|^2 + |t_{Ac}|^2 = 1$ in Eq.13 we finally

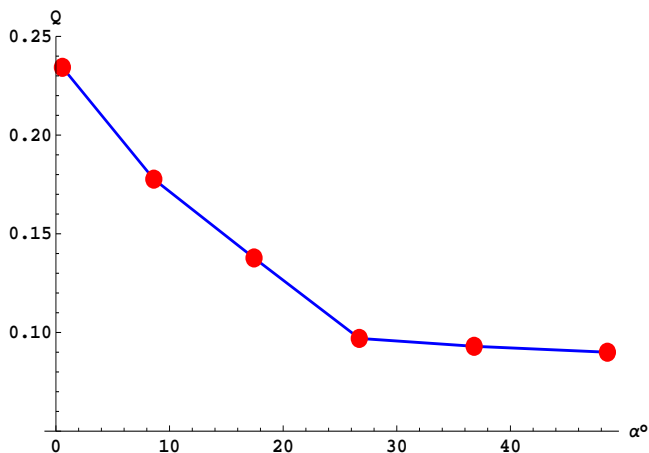


FIG. 5: (Color online) The maximum value of the pumped charge Q_{max} in units of electron charge e through the SDB structure, for pumping in $\Delta_1 - \Delta_2$ plane, is shown as a function of the incident angle α .

obtain

$$\begin{aligned}
 \mathcal{Q} = \frac{e}{2\pi} \int_0^\tau dt & \left[|r_c|^2 (\dot{\theta} \cos \alpha + \dot{\beta} \cos \alpha') \right. \\
 & + |t_c|^2 (\dot{\chi} \cos \alpha + \dot{\beta} \cos \alpha') \\
 & \left. + |t_{Ac}|^2 (\dot{\beta} - \dot{\gamma}) \cos \alpha' - \dot{\beta} \cos \alpha' \right] \quad (14)
 \end{aligned}$$

Eq.14 is the working formula for pumped charge in our case. Note that if we substitute $k_y = 0$, (*i.e.* $\alpha = \alpha' = 0$) in Eq.14, then the formula reduces to

$$\mathcal{Q} = \frac{e}{2\pi} \int_0^\tau dt \left[|t_c|^2 (\dot{\chi} + \dot{\beta}) - \dot{\beta} \right] \quad (15)$$

which is precisely the modified Brouwer's formula used in Ref.40 for the quantum wire case. In Eq.15, the first term is called the “*dissipative part*” and the second term is known as the “*topological part*” and depends entirely on the time derivative of the AR phase.

The pumped charge is obtained by using Eq.14 with Δ_1 and Δ_2 as the two pumping parameters. These two parameters are varied by periodically varying the top gate voltage which controls the Fermi energy of the electrons in the superconducting region. Thus essentially, as mentioned earlier, ϵ/Δ is varied for the two barriers periodically. Using Eq.14, we obtain the pumped charge for various parameters of the system. In Fig. 3 and Fig. 4, we show the behaviour of the pumped charge as a function of the pumping strength P and the phase difference between the two pumping parameters η respectively, for three values of k_y . Note that in Fig. 3(a), the pumped charge increases with the increase in the pumping strength P as a larger value of P corresponds to a larger pumping contour which encloses more and more of the resonance.

Note also that the $|t_c|^2 = 1$ resonance at $k_y = 0$ is not a sharp resonance; it has a finite width because it also has contribution from the “*dissipative part*” as shown in Eq.15. and is not purely topological. The “*dissipative part*” effectively reduces the pumped charge from integer values but we still obtain a fairly large value of pumped charge - where by large we mean that the pumped charge is a sufficiently large fraction of unity (roughly between 0.1 and 0.35). This is in sharp contrast to normal DB in graphene where the pumped charge²⁷ is very small (in the range of 10^{-4} , because there is no resonance due to Klein tunneling. However for oblique incidence *i.e.* $k_y \neq 0$ (see Figs. 3(b) and (c)), we obtain relatively smaller values of pumped charge as in this case normal reflection, CT, AR (and SAR) and CAR (SCAR) also contribute to Eq.14 and the interplay between all the quantum mechanical amplitudes and their phases result in smaller value of pumped charge.

In Fig. 4, we show the oscillatory behaviour of pumped charge as a function of the phase difference η between the two time varying parameters. Here also we note that we obtain smaller values of pumped charge through the SDB geometry as we vary k_y from normal incidence to oblique incidence. Note also that in Fig. 4, for all three values of k_y , the pumped charge becomes maximum around $\eta \sim \pm\pi/2$.

Finally, we also show the systematic behaviour of the maximum value of pumped charge through the SDB geometry as a function of the incident angle α of the incident electron in Fig. 5. This behaviour clearly shows that the maximum value of the pumped charge becomes smaller as we vary α from normal incidence ($\alpha = 0$) to oblique incidence ($\alpha \neq 0$).

IV. SUMMARY AND DISCUSSIONS

To summarize, in this paper, we have studied adiabatic quantum pumping through an SDB structure in graphene and have shown that in the $\Delta_1 - \Delta_2$ plane, pumped charge can be large (around 0.2- 0.3) in magnitude for normal incidence. This is in contrast to normal double barriers in graphene, where the pumped charge is small (around 10^{-4}) due to the phenomenon of Klein tunneling. We also show that in the $\Delta_1 - \Delta_2$ plane, transmission resonances ($|t_c|^2 = 1$) occur due to the formation of Andreev bound states between the two superconducting barriers. When the pumping contour encloses this $|t_c|^2 = 1$ resonance, we obtain significant amount of pumped charge for normal incidence ($k_y = 0$). However, the transmission resonances get damped as the incident angle increases due to reflection and SAR. Hence, we obtain much smaller values of pumped charge for oblique incidence. We have also studied the pumped charge through the SDB structure as a function of the pumping strength (P) and the phase difference (η) between the two pumping parameters. The most interesting study is the evolution of the maximum value of pumped charge through our pro-

posed geometry as a function of the angle of incidence of the incoming electron. This shows monotonic decrease of pumped charge as we increase the angle of incidence of the incoming electron.

Similar behaviour has also been predicted for many other systems where one studies quantum pumping through nanostructures. Integer pumped charge has been shown for pumping through quantum dots^{8–10} as well as through Luttinger liquids^{11,14,15,40}. In more recent times, similar behaviour of pumped charge has been predicted in graphene *NIS* junctions⁴¹ and in an *InAs* Josephson pump⁴⁴.

As far as the practical realization of such an SDB structure in graphene is concerned, it should be possible to fabricate such a geometry by depositing thin strips of a spin singlet superconductors (like *Al* or *Nb*) on top of a graphene sheet⁴⁵ at two places. The width of the

strips should be of the order of the superconducting phase coherence length ($10 - 15nm$ in case of *Nb*) for CT and CAR (and SCAR) to take place. In our geometry, pumped charge can be obtained by periodically varying the top gate voltage which controls the Fermi energy of the electrons in the superconducting region which amounts to varying ϵ/Δ for the two barriers periodically. The pumped current should be in the range of pico-amperes when the pumping frequency is the order of a few MHz, and should be experimentally measurable.

Acknowledgments

The work of A.S. was supported by the Feinberg Fellowship Programme at Weizmann, Israel.

-
- ¹ D. J. Thouless, Phys. Rev. B **27**, 6083 (1983).
² M. Büttiker, H. Thomas, and A. Pretre, Z. Phys. B **94**, 133 (1994).
³ P. W. Brouwer, Phys. Rev. B **58**, R10135 (1998).
⁴ M. L. Polianski and P. W. Brouwer, Phys. Rev. B **64**, 075304 (2001).
⁵ M. Moskalets and M. Büttiker, Phys. Rev. B **66**, 205320 (2002).
⁶ M. Moskalets and M. Büttiker, Phys. Rev. B **69**, 205316 (2004).
⁷ Y. Levinson, O. Entin-Wohlman, and P. Wolffe, Physica A **302**, 335 (2001).
⁸ O. Entin-Wohlman and A. Aharony, Phys. Rev. B **66**, 035329 (2002).
⁹ S. Banerjee, A. Mukherjee, S. Rao, and A. Saha, Phys. Rev. B **75**, 153407 (2007).
¹⁰ I. L. Aleiner and A. V. Andreev, Phys. Rev. Lett. **81**, 1286 (1998).
¹¹ P. Sharma and C. Chamon, Phys. Rev. B **68**, 035321 (2003).
¹² R. Citro, N. Andrei, and Q. Niu, Phys. Rev. B **68**, 165312 (2003).
¹³ E. Sela and Y. Oreg, Phys. Rev. B **71**, 075322 (2005).
¹⁴ S. Das and S. Rao, Phys. Rev. B **71**, 165333 (2005).
¹⁵ A. Agarwal and D. Sen, Phys. Rev. B **76**, 035308 (2007).
¹⁶ J. Splettstoesser, M. Governale, J. König, and R. Fazio, Phys. Rev. Lett. **95**, 246803 (2005).
¹⁷ S. K. Watson, R. M. Potok, C. M. Marcus, and V. Umansky, Phys. Rev. Lett. **91**, 258301 (2003).
¹⁸ P. J. Leek *et al*, Phys. Rev. Lett. **95**, 256802 (2005).
¹⁹ M. R. Buitelaar *et al*, Phys. Rev. Lett. **101**, 126803 (2008).
²⁰ S. P. Giblin *et al*, New J. Phys. **12**, 073013 (2010).
²¹ M. D. Blumenthal *et al*, Nat. Phys. **3**, 343 (2007).
²² K. S. Novoselov, A. K. Geim, S. V. Morozov, D. Jiang, Y. Zhang, S. V. Dubonos, I. V. Grigorieva, and A. A. Firsov, Science **306**, 666 (2004).
²³ A. K. Geim and K. S. Novoselov, Nat. Materials **6**, 183 (2007).
²⁴ A. H. Castro Neto, F. Guinea, N. M. R. Peres, K. S. Novoselov, and A. K. Geim, Rev. Mod. Phys. **81**, 109 (2009).
²⁵ S. D. Sarma, S. Adam, E. H. Hwang, and E. Rossi (2010), arXiv:1003.4731 [cond-mat.mes-hall].
²⁶ M. I. Katsnelson, K. S. Novoselov, and A. K. Geim, Nat. Phys. **2**, 620 (2006).
²⁷ R. Zhu and H. Chen, Appl. Phys. Lett. **95**, 122111 (2009).
²⁸ E. Prada, P. San-Jose, and H. Schomerus, Phys. Rev. B **80**, 245414 (2009).
²⁹ E. Prada, P. San-Jose, and H. Schomerus (2010), arXiv:1007.316 [cond-mat.mtrl-sci].
³⁰ J. Wang, Y. Wei, B. Wang, and H. Guo, Appl. Phys. Lett. **79**, 3977 (2001).
³¹ F. Zhou, Int. J. Mod. Phys. B **15**, 117 (2001).
³² M. Blaauboer, Phys. Rev. B **65**, 235318 (2002).
³³ M. Governale, F. Taddei, R. Fazio, and F. W. J. Hekking, Phys. Rev. Lett. **95**, 256801 (2005).
³⁴ F. Taddei, M. Governale, and R. Fazio, Phys. Rev. B **70**, 052510 (2004).
³⁵ J. Splettstoesser, M. Governale, J. König, F. Taddei, and R. Fazio, Phys. Rev. B **75**, 235302 (2007).
³⁶ N. Kopnin, A. S. Melnikov, and V. M. Vinokur, Phys. Rev. Lett. **96**, 146802 (2006).
³⁷ B. Wang and J. Wang, Phys. Rev. B **66**, 201305 (2002).
³⁸ B. Wang and J. Wang, Phys. Rev. B **65**, 153311 (2002).
³⁹ S. Russo, J. Tobiska, T. M. Klapwijk, and A. F. Morpurgo, Phys. Rev. Lett. **99**, 086601 (2007).
⁴⁰ A. Saha and S. Das, Phys. Rev. B **78**, 075412 (2008).
⁴¹ M. Alos-Palop and M. Blaauboer (2011), arXiv:1102.0926 [cond-mat.mes-hall].
⁴² A. Kundu, S. Rao, and A. Saha, Phys. Rev. B **82**, 155441 (2010).
⁴³ C. W. J. Beenakker, Phys. Rev. Lett. **97**, 067007 (2006).
⁴⁴ F. Giazotto *et al* (2011), arXiv:1102.4207 [cond-mat.mes-hall].
⁴⁵ H. B. Heersche, P. J. Herrero, J. B. Oostinga, L. M. K. Vandersypen, and A. F. Morpurgo, Nature **446**, 56 (2007).